Journal of Chemical Technology and Metallurgy, 60, 4, 2025, 663-672

EVALUATION OF MECHANICAL PROPERTIES, WEAR AND HARDENING POTENTIALS OF CASSAVA LEAVES (MANIHOT SPP), FeCr, AND FeMo ON CASE HARDENED DUCTILE IRON

Sylvester O. Omole[1], Abdullahi O. Adebayo[2], Ekiomoadona M. Inegbedion[1]

[1]*Metallurgical and Materials Engineering Dept.*
School of Engineering and Engineering Technology
Federal University of Technology, Akure, Nigeria, soomole@futa.edu.ng (S.O.);
ekipretty@yahoo.com (E. I.).
[2]*Materials and Metallurgical Engineering Dept.,*
Faculty of Engineering, Federal University Oye - Ekiti, Nigeria
abdullahi.adebayo@fuoye.edu.ng (A.A.).

Received 20 October 2024
Accepted 12 January 2025
DOI: 10.59957/jctm.v60.i4.2025.15

ABSTRACT

In this study ductile iron was produced using lift out crucible furnace and was "packed" case hardened with simulated carbide from Ferrochromium (FeCr), Ferromolybdenum (FeMo) mixed with graphite, and grinded cassava leaves (Manihot Spp), by heating to temperature of 850°C in the presence of snail shell as energizer, held for 2 h in the muffle furnace and were quenched in SAE 20W-50 engine oil. They were tempered at 500°C for 2h and allowed to cool in air to room temperature. Both the treated and untreated samples were characterized with metallurgical microscope. Wear and mechanical tests such as hardness, tensile and fracture toughness were carried out on treated and untreated samples. The microstructural features shows sample A treated with FeCr and graphite to have clusters of diffused carbides, that of B treated with FeMo and graphite showed finely dispersed carbide around the nodules and that of C was seen with diffused carbo-nitride compounds or cyanide finely dispersed into the structure. Sample C treated with cassava leaves has the highest hardness value and lowest wear rate, followed by sample A treated with FeCr, then sample B treated with FeMo. Sample A has a slightly higher fracture toughness and UTS than sample C.

Keywords: case hardening, diffusion, ductile iron, hardness, fracture toughness.

INTRODUCTION

Ductile iron has its graphite in the form of nodules or spheroids, which is why it is called nodular iron or spheroidal graphite iron [1]. The ductile cast iron was developed from grey cast iron by addition of magnesium into liquid iron to convert the graphite into nodules. The nodules coupled with the matrix give the iron improved properties of ductility, strength and toughness over other cast irons [2]. Generally, in cast iron the graphite shape or structure determines the type of cast iron that is produced. The shape can either be in flakes form resulting in the production of gray cast iron, spheroidal shape or nodular shape results in the production of ductile iron also known as spheroidal graphite iron or nodular cast iron, randomly oriented and elongated graphite with structures between gray cast iron and ductile cast iron gives rise to compacted graphite iron and white cast iron has the graphite in carbide form [3]. The nodular graphite shape in ductile cast iron therefore confers superior properties of ductility and low crack initiation as compared to other types of cast iron [4].

One of the properties of ductile iron that made it useful in the industry is its wear resistance, but in a severe condition, the wear resistance properties soon fade out [5]. Therefore, there is the need to improve on the wear resistance especially at the working surface. Various conventional alloys are subjected to wear and sudden fracture when utilized under different conditions which involve abrasion, grinding media and high temperature tribological environment [6]. Meanwhile, some of these materials may have been produced by alloying with carbide stabilizing elements such as chromium, manganese, molybdenum and so on. This type of high alloyed materials may produce carbides' structure in the entire part of the products, thereby making machining very difficult to carry out on the product [7, 8]. However, the wear resistance, fracture parameter and the oxidation tendency of the iron need to be improved upon even after alloying. This will be important when used to transport fluids where there will be chemical interaction and high velocity transportation. Also useful in grinding media such as in minerals and ores processing. One basic means of achieving adequate hardness and high wear resistance in a material especially, at the surface and as well preserve toughness at the core of the material is by surface /case hardening, this leads to enhancement of wear resistance of the part at the surface and maintaining a high toughness at the core [9].

Cassava leaves is one of the agro wastes that is available in large quantity in most Africa countries in an unutilized state. They are often discarded after harvest of the cassava tuber. Several researchers such as Ibironke et al. [10], Ampaw et al. [11], Adetunji et al. [12], Taiwo et al. [13], Arthur and Azeko [14] and so on, had utilized this cassava leaves as a means of carbo-nitriding treatment to achieve high wear resistance. However, it had not been proven maybe it will be able to compete with some ferroalloys when they are all used for case hardening treatment. Again, to achieve effective results in case hardening treatment energizer/ enhancer are often used.

Ampaw et al. [11] used barium carbonate as enhancers, Effendi et al. [15] use of 30 % calcium carbonate ($CaCO_3$) with activated carbon to achieve carburized product. Ihom et al. utilized eggshell waste as an enhancer in the carburization of steel [16]. But in this research, snail shell which are often discarded as a waste is utilized to achieve an energized reaction as it contained calcium. Energizer in this reaction can be likened to a catalyst which will help to speed up or enhance the diffusion of the desired elements into the treated material.

This research aims at studying the potency of cassava leaves for carbo-nitriding treatment and then evaluate the results and compare with that of simulated environment of chromium carbide and molybdenum carbide used for the case hardening treatment. The effectiveness of each treatment was quantified by the result of mechanical and wear properties of the ductile iron achieved. This is in a view to develop structure that will enhance wear resistance and mechanical properties in the iron at a cheaper rate from the agro wastes.

EXPERIMENTAL

Materials

Materials utilized for this research are gray cast iron, graphite, ferrosilicon (72 %), ferrosilicon magnesium (with 45 % silicon and 5 % magnesium), limestone as flux, calcium carbide as desulphuriser, ferrochrome (65 % Cr), ferromolybdenum (72 % Mo) and processed cassava (manihot spp) leaves as a source of agro cyanide.

Production of ductile cast iron

Gray cast iron scraps was melted in a lift out crucible furnace using black oil as a source of fuel. The charge was prepared to have copper content in the range 0.2 - 0.4 %, following a standard procedure of charge calculation in accordance with Wang et al. [17]. The charge was heated to temperature of 1350^{o}C before addition of calcium carbide in accordance with Omole et al. [4], in other to reduce sulphur in the melt. The desulphurised melt was superheated to temperature of 1420^{o}C, tapped from the crucible into a ladle that contained FeSiMg according to sandwich treatment method. During nodularisation treatment FeSi was added to inoculate the melt. Nodularised melt was cast into prepared mould of a cylindrical pattern ø16 mm by 150 mm length. The casting was allowed to cool to room temperature in the mould, then knocked out of the mould and cleaned.

Chemical composition determination

Chemical composition of the produced ductile iron was done using Tasman absorption spectrometric analyser. The surface of the sample was first prepared by grinding with emery paper to make it flat. The spectrometer makes use of argon gas to burn the surface of the prepared iron sample for content analysis. Average of three readings having variability of at most ± 8 % was taken to determine the composition of the ductile iron.

Machining of mechanical test samples

Samples for mechanical tests - tensile, hardness, fracture toughness and metallographic studies was machined out on Colchester Triumph 2000 series lathe machine, with different specifications for each test sample. Tensile sample was machined to gauge diameter of 5 mm, gauge length of 40 mm as shown in Fig. 1a. The fracture toughness sample is a circumferential notch tensile (CNT) specimen with notch diameter of 4.2 mm, notch angle of 60° and gauge diameter of 5 mm, the sample is shown in Fig. 1b. Samples for microstructure and hardness were machined to diameter of 12 mm by 12 mm long.

Preparation of additives for case hardening treatment

Fresh cassava (manihot spp) leaves were plucked and sun dried for some days, charged in ball mill with adequate number of balls for grinding, it was grinded till appreciable powder was obtained. Ferrochrome containing 65 % chromium, ferromolybdenum containing 72 % molybdenum and graphite were crushed using pulveriser. They were later taken to ball mill at different time and adequate number of balls were introduced, ground to obtain powder form of the ferroalloys and graphite. Snail shells were dried and pulverized, then charged into ball mill and was grinded. All the prepared powder were graded to - 355 µm. These materials were prepared as follows: (a) 60 % w/w ferrochrome with 30 %w/w graphite and 10 % w/w snail shell as A. (b) 60 % w/w ferromolybdenum with 30 % w/w graphite and 10 % snail shell as B and (c) 90 % cassava leaves powder with 10 % w/w snail shell as C.

Case hardening process

The treatment was done in three different ceramic lined metallic crucible. The crucible and the samples labelled A contained ferrochrome and graphite with snail shell for treatment, that labelled B contained ferromolybdenum and graphite with snail shell for treatment and the last one labelled C contained processed cassava leaves as a source of cyanide with snail shell. The pulverized snail shell was added as an enhancer or energizer into each treatment portion in accordance with Ihom et al. [16], Effendi et al. [15]. The essence of lining the metallic crucible is to prevent the diffusion of the additives for treatment into the metallic crucible.

They were all heated to temperature of 850°C in a muffle furnace held for two hours, and the contents in each crucible was quenched in SAE 20W-50 engine oil then allowed to cool to room temperature. The treated samples A, B and C was heated again to 500°C held for 2h and allowed to cool in air, which is a tempering treatment, to impact toughness and relieve the treated samples of residual stresses.

Microstructural examination

Samples for microstructural test was separated after the case-hardened treatment. They were prepared through series of metallographic processes, starting from grinding using 120 grits of emery paper, followed by 320 grits, 400 grits and ended the grinding with 600 grits of emery paper. Polishing started with 800 grits of paper, then 1000 grits and 1200 grits of emery paper. Further polishing was done using 2000 grits of paper and final polishing was done with 5 mm diamond paste on polishing cloth. Grinding and polishing was also done on the control sample tagged sample D which was not case-hardened. They were etched with nital (2 % nitric acid (HNO_3) mixed with 98 % ethanol). Etching was done by the application of etchant on the polished surface for 15 sec, swabbed in water and cleaned with cotton wool. The microstructure of the samples was viewed using Omax metallurgical microscope. Micrographs were taken both before etching and after etching the samples.

Mechanical properties test

The mechanical tests conducted on all the samples are hardness, tensile and circumferential notch tensile for the determination of the fracture toughness of the samples.

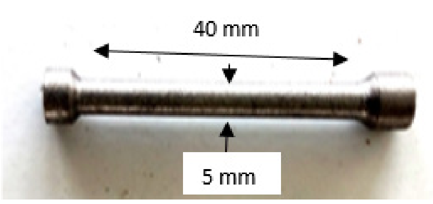

a)

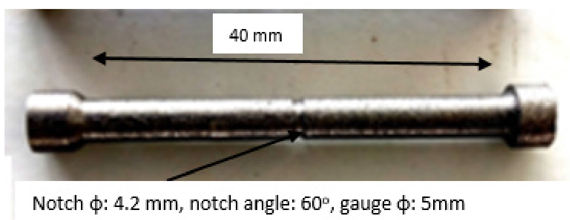

b)

Fig. 1. Tensile and circumferential notch tensile specimen samples: (a) tensile sample; (b) circumferential notch specimen.

Hardness test

The prepared sample was placed on Brinell hardness tester having a spherical carbide ball indenter of 10 mm diameter. The indenter was pressed with a 1 kN load into the surface of the sample and allowed to stay for 12 min as dwell time, to obtain sufficient indentation that will achieve accurate reading. This is in accordance with ASTM E10 [18]. After the 12 min dwell time the value of the hardness measurement was taken, and the indenter was removed. The reading was taken at three different spots on the sample to compute the average hardness.

Tensile test

Tensile test was carried out on Instron series - 3369 tensile testing machine with crosshead speed of 5 mm per minute. Samples for the test were machined to gauge length of 40 mm and gauge diameter of 5 mm, placed on the tensile machine and pulled at a quasi-static strain rate of 10^{-3}/s to fracture the samples. Data generated by the machine was collected and used to compute the tensile behaviour of both the treated and untreated materials.

Fracture toughness test

Circumferential notch tensile specimens (CNT) were used for the evaluation of the fracture toughness of all the ductile iron samples. This is in accordance with Alaneme et al. [19], Omole et al. [20]. Notch specimens were machined to gauge length of 40 mm, gauge diameter of 5 mm, notch diameter of 4.2 mm and notch angle of 60°. They were subjected to pull to fracture, with a strain rate of 10^{-3}/s. The fracture toughness of the material was then evaluated using the relation in Eq. (1) in accordance with Dieter [21].

$$\mathrm{Kic} = \frac{Pf}{\mathrm{D}^{3/2}}\left[1.72\left(\frac{\mathrm{D}}{d}\right) - 1.27\right] \tag{1}$$

where D is the gauge diameter, d is the notch diameter. In accordance with Nath and Das, the validity of the determined fracture toughness values can be obtained using the relationship in Eq. (2) [22].

$$\mathrm{D} \geq \left(\frac{Kic}{\sigma y}\right)^2 \tag{2}$$

where σy the yield strength and Kic is the fracture toughness evaluated.

Wear test

Anton Paar Tribometer (TRB) machine which is based on pin-on-disk was used to evaluate the wear parameter in this study. The machine consists of stainless steel ball indenter having diameter of 10 mm. Load of 10 N was applied on the test specimens with speed of 7.85 cm s^{-1} for a period of 30 minutes on each test. Volumetric wear rate was estimated according to Ampaw et al. [11] Agbeleye et al. [23]. This is done by calculating the wear volume and specific wear rate from the mass of material removed from contact surface of the specimen. Those parameters that can be calculated are expressed in Eqs. (3) to (6).

$$Sliding\ distance = Velocity\left(\frac{m}{s}\right) \times\ time(s) \tag{3}$$

$$Wear\ volume = \frac{wear\ mass}{Density} \tag{4}$$

$$Specific\ wear\ rate = \frac{Wear\ volume}{Sliding\ distance \times force\ Applied} \tag{5}$$

$$Wear\ rate = \frac{Wear\ volume}{Sliding\ distance} \tag{6}$$

RESULTS AND DISCUSSION

Chemical composition of the ductile iron produced

The chemical composition of the produced ductile iron before case hardening treatment (sample D) is presented in Table 1. The composition shows enough % carbon and silicon that gives the cast iron carbon equivalent value (CEV) of 4.23 % as obtained using equation 7, the value of the CEV is close to ductile iron eutectic point of 4.3 %. The carbon and silicon are also enough to aid the production of nodules in the ductile iron in accordance with Ochulor et al. [24]. Residual magnesium of 0.083 obtained in the casting is also enough to sustain the nodules in the casting during solidification [25].

$$CEV = TC + \frac{\%Si + \%P}{3} \tag{7}$$

where TC = % total carbon, Si = % silicon and P = % phosphorus.

Microstructure evaluation

Micrograph of treated and untreated ductile iron are presented in Figs. 2 - 5 in unetched and etched with 2 % nital at magnification of X 100. The base ductile iron (sample D) is seen to contain ferrite and pearlite, with more visible quantity of pearlite structure than ferrite. This can be recognized from the etched samples. Samples A, B and C are seen to have small size of nodules in Fig. 2, 3 and 4 compared to sample D that is control sample.

This can be attributed to the heat treatment in which the rate of heat removal from the case-hardened samples was rapid during quenching, this can give rise to the reduction of sizes of the nodules present in the material [26]. It can be seen that the diffusion of carbides (chromium carbide, molybdenum carbides) and cyanides are formed within the interstices of the structure, and some were seen to be attracted to the nodules as can be seen in etched samples A, B and C of Figs. 2 - 4. However, they did not take the shape of nodules but are seen around the nodules. Previous similar works such as Yordanov et al. [27], Su et al. [28], Taiwo et al. [13] ascertained the presence of carbides and cyanide in such processes which further boost this discussion on the carbide pattern. Higher magnification (X 400) of micrographs of sample A to D are presented in Fig. 6.

Mechanical properties results

Hardness

The hardness values of both the treated and untreated ductile iron samples are shown in Table 2. That of sample C was observed to be the highest with 16.24 % increase in hardness compared to the sample D which is the control sample (untreated). This may be due to ability of cassava leaves to break down at ease with high enthalpy change. It will easily release out carbon and nitrogen at high temperature, as it is an agricultural waste which can act as fuel during combustion and release out its elements

Table 1. The average chemical composition of the produced ductile iron.

Elements	%C	%Si	%Mn	%Mo	%Cu	%Mg	%S	%P
Sample D	3.52	2.10	0.45	0.12	0.26	0.083	0.030	0.022

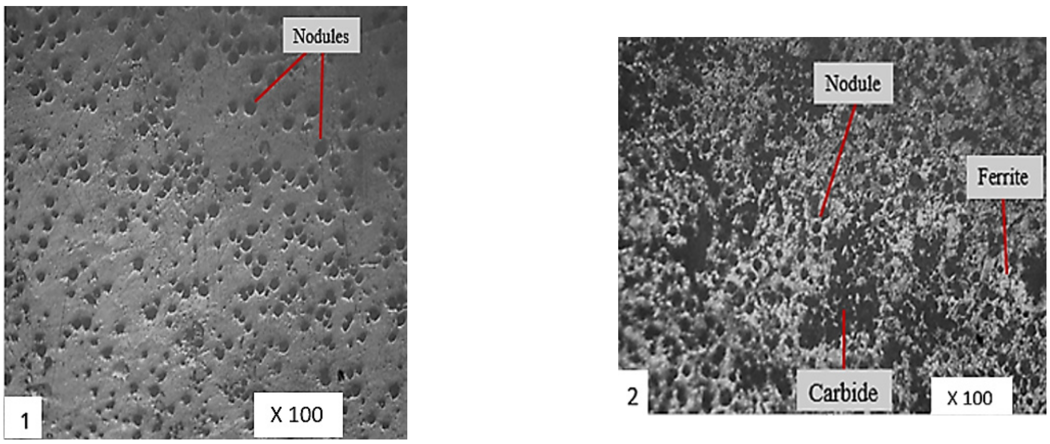

Fig. 2. Microstructures of sample A (1 is unetched and 2 is etched sample).

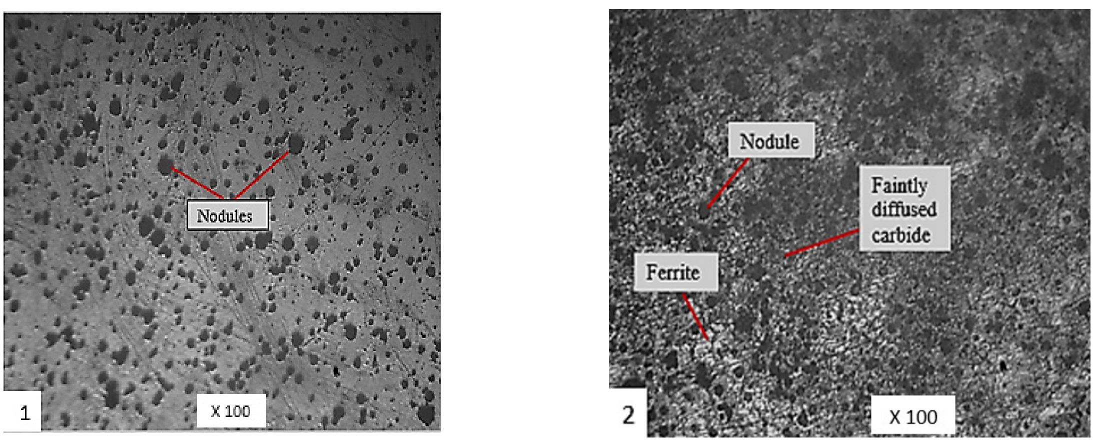

Fig. 3. Microstructures of Sample B (1 is unetched and 2 is the etched sample).

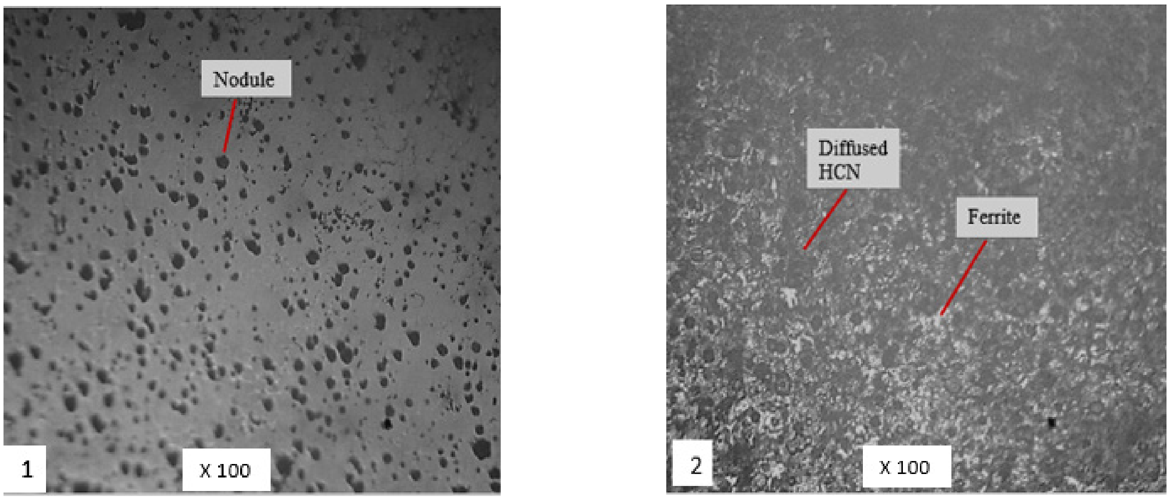

Fig. 4. Microstructures of Sample C (1 is unetched and 2 is the etched one).

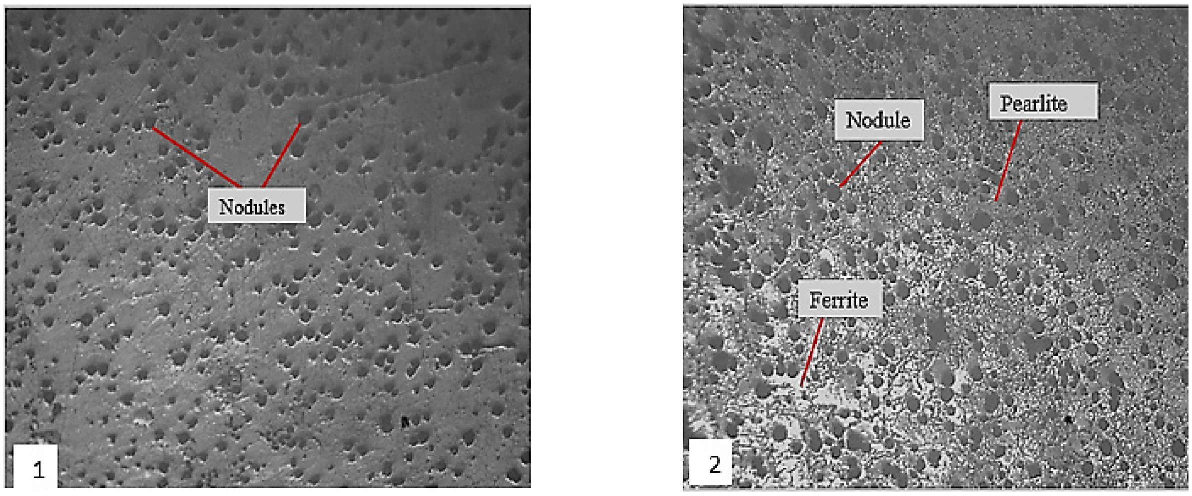

Fig. 5. Microstructures of Sample D (1 unetched and 2 is the etched sample).

to diffuse easily at high temperature. Therefore, diffusion potential of cassava leaves to the sample is perceived to be higher than those of chromium and molybdenum with graphite.

The hardness value of sample A closely followed that of sample C with 13.20 % increase in hardness value in comparison with sample D. It can be said that chromium is more effective than molybdenum because chromium is said to have higher diffusion rate (among some tested ferroalloys) in BCC crystal structure materials such as cast iron, and the diffusion coefficient increases with increase in temperature [29]. However, chromium couldn't give result higher than cassava leaves but higher than that of molybdenum. It can also be inferred that the reduction in effectiveness of the ferroalloys particularly Mo to perform up to cassava leaves may be due to kinetics required at solid state to enable graphite react with ferrochrome and ferromolybdenum at high temperature to form their carbides, even despite the reaction was in the presence of snail shell (source of calcium) which acts as an enhancer in accordance with Ihom et al. [16], etc.

Stress - strain

The tensile stress - strain curves of all the samples are shown in Fig. 7. From the graphs and the accompanied data, some of the behaviours of the ductile iron samples are expressed by parameters such as ultimate tensile strength, percentage elongation. Sample A has the

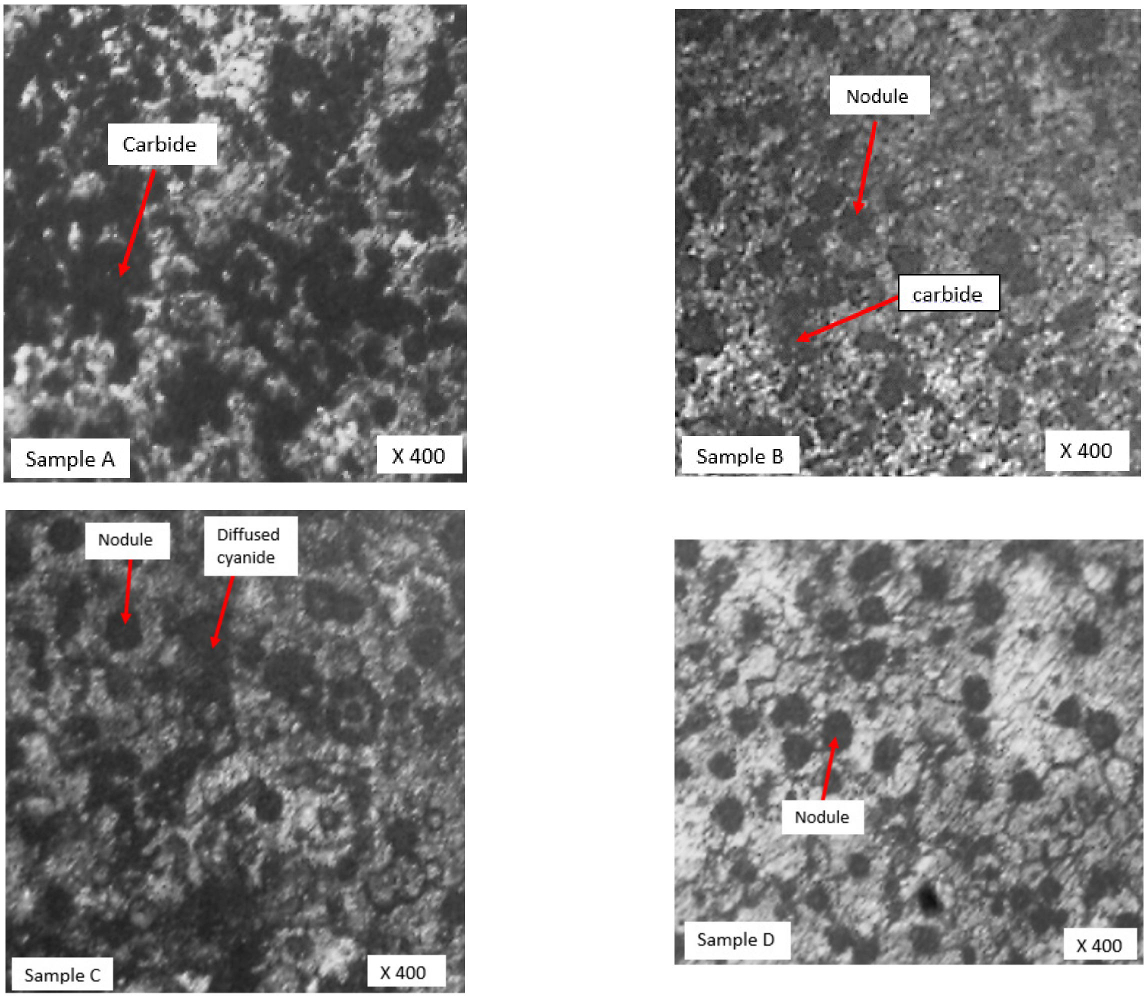

Fig. 6. Micrographs of samples A to D in X 400 (etched in 2 % nital).

Table 2. Hardness values of treated and untreated ductile iron.

Sample	Brinell Hardness (BHN) (dwell time of 12 min.)	Average Hardness Value (BHN)
A	152.45 143.67 147.29	147.80 13.2 % increase
B	133.65 134.54 137.81	135.33 3.65 % increase
C	156.78 148.47 150.06	151.77 16.24 % increase
D	132.74 128.35 130.62	130.57 control sample

highest work hardening response because of its highest ultimate tensile strength (UTS).

Ultimate tensile strength and percentage elongation

The variation of ultimate tensile strength of both treated and untreated samples is presented in Fig. 8 that of percentage elongation is shown in Fig. 9. It is seen that sample A has the highest ultimate tensile strength, and the control sample (D) has the highest elongation and strain value. However, sample C treated with cassava leaves and having highest hardness value still competed with other samples, although it did not possess the highest UTS. Its performance in this test might be due to the possession of appreciable fracture toughness in comparison with other samples. However, sample D was observed to have the highest percentage elongation. This is because it is untreated sample, and it would still possess the highest ductility in a control state. This is also seen on the stress - strain curve that the sample D possesses the highest strain value, hence the highest ductility. Other samples such as A and C are closely following each other in elongation value, and it confirmed that both samples still maintain some appreciable level of ductility also.

Fracture toughness

The variation of the fracture toughness of all the samples is shown in Fig. 10. Sample A treated with chromium to form carbide has the highest fracture toughness, this implies that chromium carbide has higher toughen-ability than other additives used for treatment. Although it is closely followed by sample C treated with cassava leaves. Therefore, cassava leaves have not perform below what can be recommended for case hardening treatment. Even sample D that was not treated was competing with that of Sample B treated with molybdenum. So, under this treatment pattern the molybdenum with graphite did not perform to expected level like other additives used.

Wear result

The wear mass obtained from the wear test of each sample was used to compute the sliding distance, wear volume and wear rate using Eq. (3), (4) and (6). Sample C treated with cassava leaves has the lowest wear volume and it has the lowest wear rate. Table 3 shows the

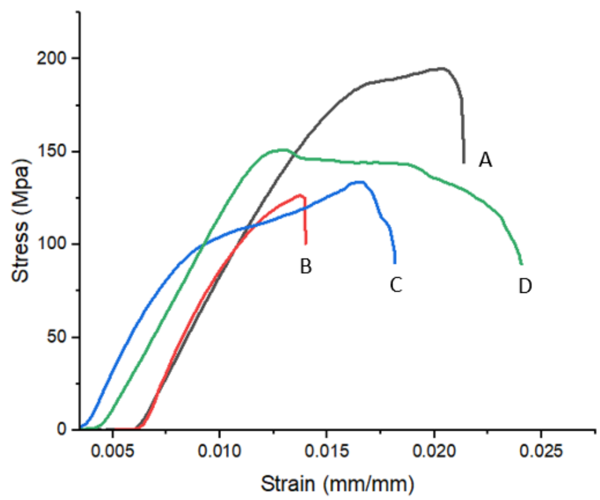

Fig. 7. Stress - strain curves of the samples.

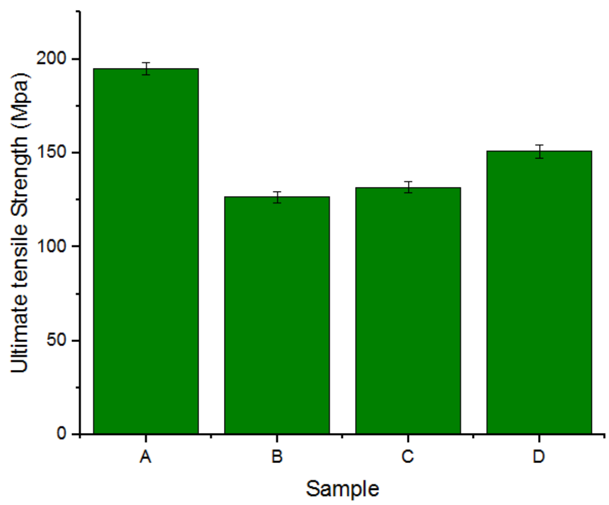

Fig. 8. Variation of the ultimate tensile strength of the sample.

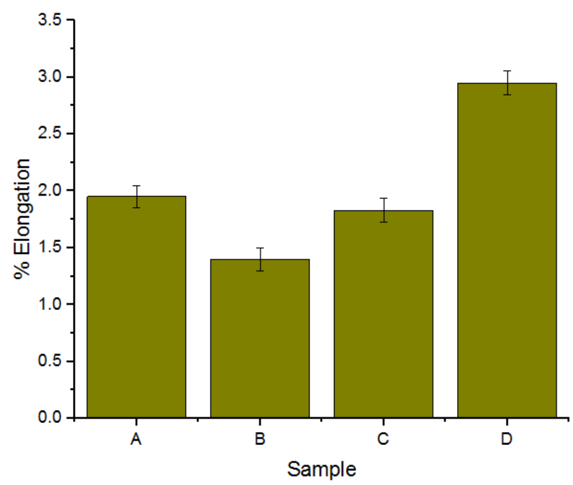

Fig. 9. Variation of percentage elongation of the samples.

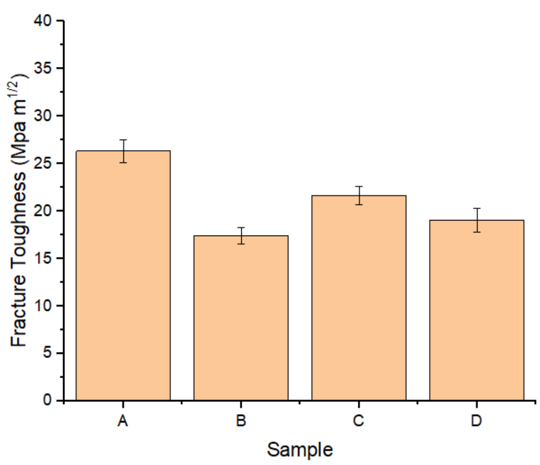

Fig. 10. Fracture toughness of all the samples.

Table 3. Values of wear volume wear mass and wear rate of all the samples.

Sample	Wear mass, g	Wear volume, cm^3	Wear rate, cm^2
A	0.032	4.066×10^{-3}	2.884×10^{-7}
B	0.035	4.447×10^{-3}	3.154×10^{-7}
C	0.012	2.795×10^{-3}	1.982×10^{-7}
D	0.044	5.591×10^{-3}	3.965×10^{-7}

variation of these parameters in the samples considered. It was discovered that the higher the hardness value, the lower the wear rate amongst the samples considered. From the wear results obtained, it suggests that cassava leaves possess higher potentials for hardening treatment through case hardening than the ferroalloys used. This can be attributed to the ability of the cassava leaves to burn out faster and diffuse into the metallic sample.

CONCLUSIONS

Ductile iron produced contains some pearlite matrix phase in the iron. The production reflected near eutectic composition of ductile cast iron. The produced ductile iron was case hardened in cassava leaves, simulated environment of ferrochrome and graphite and ferromolybdenum and graphite to produce their carbides to diffuse into the ductile iron. From the tests carried out, the following can be deduced:

- The ductile iron produced is hypoeutectic iron due to its carbon equivalent value of 4.23 % although very close to eutectic point of 4.3 %.
- Sample C treated with cassava leaves has the highest hardness value and the lowest wear rate of all the samples.
- Sample A has slightly highest fracture toughness that is closely followed by sample C treated with cassava leaves, highest UTS was also observed in sample A.
- The control sample (D) has the highest elongation with highest strain value of all the samples, this confirms the retention of its ductility in the as cast form since it was not case hardened.
- In all the test results obtained, sample B which was treated with Molybdenum and graphite has the lowest result values.
- As a result of oil quenching of the treated samples, the structure, nodules and matrix of the ductile iron are slightly modified, which is also in accordance with Yadav et al. [26].

Acknowledgement

The authors acknowledge the permission of the Departments of Metallurgical and Materials Engineering, Federal University of Technology, Akure and Federal University Oye Ekiti, for the use of Laboratories and equipment in the Departments for the research.

Authors' Contributions: *S.O.: Conceptualization, literature review, analysis and discussion, manuscript draft preparation and editing. A.A.: Literature review, reviewing the manuscript and editing. E.I.: Literature review, typesetting and editing. All authors participated in writing the article.*

REFERENCES

1. A.O. Adebayo, K.K, Alaneme, A. Oyetunji, Structural characterization and mechanical properties of rotary melting furnace processed aluminium alloyed ductile irons, J. Taibah Univ. Sci., 13, 1, 2019, 248-257.
2. M. Soliman, A. Nofal, H. Palkowski, Alloy and process design of thermo-mechanically processed multiphase ductile iron, Mats Des., 27, 2015. 450-465.
3. C. Fragassa, A. Pavlovic, Compacted and spheroidal graphite iron: experimental evaluation of Poisson's ratio, FME Transaction 4, 2016, 327-332.
4. S.O. Omole, A. Oyetunji, K.K. Alaneme, P.A. Olubambi, Structural characterization and mechanical properties of pearlite enhanced micro-alloyed ductile irons, J. King Saud Univ. Eng. Sci., 32, 2020, 205-210.
5. M.H. Sohi, M. Ebrahimi, H.M. Ghasemi, A. Shahripour, Microstructural study of surface melted and chromium surface alloyed ductile iron, Appl. Surf. Sci., 258, 2012, 7348-7353.
6. D. Fernandino, R. Boeri, Quantification of the fracture surface profiles resulting from different loading conditions on ductile irons, Proced. Mat.

Sci., 8, 2015, 108-116.
7. A.S. Elkem, Overview of alloying elements and their effects in grey iron. Technical information, Publication of Elkem AS Foundry products, Oslo, Norway. 12A, 2011, 1-8.
8. X-R. Chem, Q-J. Zhai, H. Dong, B-H. Dai, H. Mohrbacher, Molybdenum alloying in cast iron and steel, Adv. Manuf., 8, 2020, 3-14.
9. N. Fonseca, D.S. Guterres, The effects of chill thickness to microstructure and surface hardness layer on specimen ductile iron, The 4th International conference on materials and metallurgical engineering and technology (ICOMMET), Faculty of Engineering, Diponegoro University Tembalang, Semarang, Indonesia, 2020.
10. O.J. Ibironke, A. Falaiye, , T.V. Ojumu, E.A. Odo, O.O. Adewoye, Case - depth studies of pack cyaniding of mild steel using cassava leaves, Mats. Manuf. Processes, 19, 5, 2004, 899-905.
11. E.K. Ampaw, E.K. Arthur, O.O. Adewoye, A.R. Adetunji, S.O.O. Olusunle, W.O. Soboyejo, Carbonitriding “pack cyaniding” of ductile irons, Adv. Mat. Resear., 1132, 2016, 330-348.
12. A.R. Adetunji, B.E. Atta Daniel, D.A. Pelemo, O.A. Olasupo, M.O. Adeoye, O.O. Adewoye, Metallographic studies of pack cyanided mild steel using cassava leaves, Mats. Manuf. Processes, 23, 2008, 1-6.
13. T.A. Taiwo, O. S. Seidu, J.K. Akinluwade, R.A. Adetunji, A.D. Isadare, Characterisation of cassava cyanide on heat treated ductile cast iron, J. Mats. Sci. Res. Rev., 1, 4, 2018, 1-12.
14. E. K. Arthur, S. T. Azeko. Surface hardening of ferrous materials with cassava (Manihot spp.) waste: A review, Scientific African, 9, 2020, e00483, 1-11.
15. S. Effendi, Firdaus., Karmin., Romli., O.F. Homzah, Y.E. Fernandes, Effects of carburizing processes nodular cast iron with variations in temperature, time and cooling system, J. Phys. Conf. Series, 1500, 2020, 1-7.
16. P.A. Ihom, G.B. Nyior, I.J. Nor, N.J. Ogbodo, Investigation of egg shell waste as an enhancer in the carburization of mild steel, Am. J. Mat. Sci., Eng., 1, 2, 2013, 29-33.
17. Y. Wang, F.S. Cannon, M. Salama, J. Goudzwaard, J.C. Furness, Characterization of hydrocarbon emissions from green sand foundry core binders by analytical pyrolis, Environmental Science and Technology, 41, 2007, 782-792.
18. ASTM E10. Standard test method for Brinell hardness of metallic materials, ASTM International, West Conshohocken, PA 19428-2959, USA.
19. K.K. Alaneme, B.O. Ademilua, M.O. Bodunrin, Mechanical properties and corrosion behavior of aluminium hybrid composites reinforced with silicon carbide and bamboo leaf ash, Tribology in Industry, 35, 1, 2013, 25-35.
20. S.O. Omole, A. Oyetunji, K.K. Alaneme, P.A. Olubambi, Fracture touhness and tribological wear behaviour of micro alloyed pearlitic - ferritic ductile cast iron, Tribology in industry, 40, 4, 2018, 584-593.
21. G.E. Dieter, Mechanical Metallurgy, New York, Mcgraw - Hill, 1992.
22. S.K. Nath, U.K. Das, Effects of microstructure and notches on the fracture toughness of medium carbon steel, J. Naval Architec. Marine Eng., 3, 2006, 15-22.
23. A.A. Agbeleye, D.E. Esezobor, S.A. Balogun, J.O. Agunsoye, J. Solis, A. Neville, Tribological properties of aluminium-clay composites for brake disc rotor applications, Journal of King Saud Univ. Sci., 32, 1, 2020, 21-28.
24. E.F. Ochulor, S.O. Adeosun, M.O.H. Amuda, S.A. Balogun, Strength characteristics of inoculated and nodularized thin wall ductile iron castings, J. Min. Mater. Charact. Eng., 3, 2015, 94-105.
25. N.S. Tiedje, Solidification, processing and properties of ductile cast iron. Institute of Materials, Minerals and Mining, Maney, 2010, 505-514.
26. D. Yadav, L.P. Singh, A. Kumar, A study of heat treatment effects on nodular iron, Journal of Emerging Technologies and Innovative Research, 5, 10, 2018, 1-17.
27. B. Yordanov, D. Krastev, A. Davidkov, K. Klyavkov, Formation of molybdenum carbide during carbidization of molybdenum chips with powdered carbon at electrothermal rotary bed condition, J. Chem. Technol. Metall., 49, 1, 2014, 40-44.
28. X. Su, S. Zhao, H. Sun, X, Yang, P. Zhang, Chromium carbide coatings produced on ductile cast iron QT600-3 by thermal reactive diffusion in fluoride salt bath: growth behavior, microstructure evolution and kinetics, ceramic international, 45, 1, 2019, 1196-1201.
29. S. Zhang, H. Zhang, H., Zhang, X. Zhao, Y. Li, Study on diffusion kinetics and law of chromium on the surface of low carbon steel. Coatings 13, 1, 2023, 98.